Supporting Information

Nonstoichiometric Copper Chalcogenides for Photo-activated Alkyne/Azide Cycloaddition

Hong Yan Zou, [a‡] Ming Xuan Gao, [b‡] Tong Yang, [a] Qiao Ling Zeng, [a] Xiao Xi Yang, [a] Feng Liu, [c] Mark T. Swihart, *[d] Na Li *[c] and Cheng Zhi Huang *[ab]

[a]Key Laboratory of Luminescent and Real-Time Analytical Chemistry, Ministry of Education, College of Pharmaceutical Sciences, Southwest University, Chongqing 400715, China.

[b]Chongqing Key Laboratory of Biomedical Analysis, Chongqing Science & Technology Commission, College of Chemistry and Chemical Engineering, Southwest University, Chongqing 400715, China.

[c]Beijing National Laboratory for Molecular Sciences, Key Laboratory of Bioorganic Chemistry and Molecular Engineering of Ministry of Education, College of Chemistry and Molecular Engineering, Peking University, Beijing 100871, China.

[d]Department of Chemical and Biological Engineering, University at Buffalo (SUNY), Buffalo, NY 14260-4200, USA.

‡These authors contributed equally in this work.

*E-mail: swihart@buffalo.edu (S. M. T.); lina@pku.edu.cn (L. N.); chengzhi@swu.edu.cn; (H. C. Z)

SUPPORTING INFORMATION INDEX

4. REFERENCES

1. EXPERIMENTAL SECTION

1.1 General Information

All reagents and solvents were obtained from standard commercial sources. The size and morphology of copper chalcogenides were characterized by TEM using a Tecnai G2F20S-TWIN microscope (FEI, USA). Scanning electron microscopy (SEM) images were captured using an S-4800 scan electron microscope (Hitachi, Japan). The powder XRD pattern was determined on an XRD-7000 operated at 40 kV and 20 mA with a 2θ range from 20° to 75° with Cu Kα radiation source. The X-ray photoelectron spectroscopy (XPS) analysis was conducted using an ESCALAB 250 X-ray photoelectron spectrometer (Thermo, USA). The samples for XPS were prepared by deposition of a nanocrystal suspension in water onto a Si substrate. Inductively coupled plasma-atomic emission spectroscopy (ICP-AES) analysis was conducted using a TPS-7000 spectrometer (Puxi, Beijing, China). UV−vis−NIR absorption spectra were obtained using a Hitachi U-3600 spectrophotometer with the nanoparticles dispersed in the synthesis reagents. Nuclear magnetic resonance (NMR) spectra were acquired on an AVANCE III 400 MHz Superconducting Fourier NMR spectrometer. Chemical shifts were referenced to the residual solvent peak. MS spectra were recorded on an Autoflex speed MALDI-TOF/TOF mass spectrometer. A Fourier transform infrared (FT-IR) spectrophotometer (FTIR-8400S, Shimadzu, Japan) was employed to measure the FT-IR spectra.

1.2 Synthesis of $Cu_{2-x}S_ySe_{1-y}$ nanocrystals

A simple one-pot wet chemical method was developed for the synthesis of heavily doped alloyed $Cu_{2-x}S_ySe_{1-y}$ nanocrystals (CuCNCs). Typically, 1 mL of 10 mg mL^{-1} polystyrene sulfonate (PSS, MW 70 kDa) and 5.5 mL water were added to a round-bottom flask and then 0.5 mL of 0.4 M Vc and 1 mL of a mixture of 0.2M Na_2S and 0.2M SeO_2 (mixed in rations of 1:0, 2:1, 1:1, 1:2, and 0:1) were added successively. After 10 min, a mixed solution of 1 mL 0.4 M $CuSO_4 \cdot 5H_2O$ and 1 mL 0.4 M ascorbic acid were added under vigorous stirring. The resulting mixture was stirred vigorously at 30°C for 0.5 h, then at 45 °C for 10 h to obtain a dark green dispersion. The dispersion was centrifuged at 10000 rpm for 10 min to collect the CuCNCs, which were then redispersed in water and further purified by dialysis using a 10 kDa dialysis membrane for 24h. The purified CuCNCs were stored in 20 mL water at 4°C for later use. The amount of

CuCNCs was quantatified by freeze-drying using Coolsafe 110-4PRO, Gene Company Limited (~0.35 mg/mL for N3, corresponding to 2.8 μmol/mL in terms of $Cu_{1.12}S_{0.55}Se_{0.45}$ formula units).

1.3 *Nonstoichiometric CuCNCs catalyzed click reactions*

In a glass vial equipped with a magnetic stir bar, approximately 0.07 μmol of CuCNCs (25 μL of the CuCNC dispersion, with CuCNC concentration as quantified by freeze-drying and weighing, e.g. ~0.35 mg/mL or 28 μmol $Cu_{1.12}S_{0.55}Se_{0.45}$ per mL for N3) in solvent (1 mL), was added to 0.25 mmol of benzyl azide and 0.45 mmol of phenyl acetylene and the reaction mixture was stirred at 25 °C. Reaction progress was monitored by TLC until the azide had been completely consumed. The crude reaction mixture was worked up with acetone, then centrifuged and filtered through filter paper to remove the catalyst. The filter paper was further washed with EtOAc to ensure complete transfer. Pure click products were obtained by column chromatography (silica gel column, mixture of aether petrolei/ethyl acetate=5:1 as mobile phase).

1.4 *Recyclability of the nonstoichiometric CuCNCs for the click reactions*

The recyclability of the nonstoichiometric copper chalcogenides as catalysts was investigated as follows: After phenyl acetylene and benzyl azide were stirred for 10 min, the used nanocystals recovered from a prior experiment were added. Subsequently, the reaction mixtures were irradiated under UV with stirring. The progress of the reaction was again monitored by TLC. After one run of the reaction was completed, the reaction mixture was diluted in acetone and centrifuged. The solution containing the product was removed, leaving behind the nanocrystal precipitate.

1.5 *In vitro cytotoxicity of CuCNCs.*

Hep-2 cells were added in the 96-well microtiter plate (1×10^5 cells per well) and cultured in Roswell Park Memorial Institute (RPMI)1640 medium supplemented with 2% fetal bovine serum at 37°C in a humidified incubator of 5% CO_2 for 24 h before the experiments. whereafter, the cells were incubated with complete medium containing the $Cu_{2-x}S_ySe_{1-y}$ NCs (sample N3) after different irradiation at a series of concentrations (28, 2.8, 0.28 μM) at 37 °C with 5% CO_2 for further 24 h and then they were rinsed with sterilized PBS

2. THEORETICAL SECTION

2.1 Calculation of band gap energy

The band gap energies of semiconductors can be estimated by using the Tauc plot,[1]

$$\alpha h\upsilon = A(h\upsilon - E_g)^2 \quad \text{(S1)}$$

Where α represents the absorption coefficient, υ is the light frequency, E_g is the band gap energy, A is a constant.

2.2 Theoretical modeling of the LSPR of the CuCNCs

The extinction spectra of $Cu_{2-x}S_ySe_{1-y}$ NCs can be theoretically calculated using the quasi-static approximation of Mie theory.[2-6] For spherical particles, the extinction cross section C_{ext} is given by equation S2

$$C_{\text{ext}} = C_{\text{abs}} + C_{\text{sca}} = \frac{24\pi^2 R^3 \varepsilon_{\text{m}}^{3/2}}{\lambda} \frac{\varepsilon_2}{(\varepsilon_1 + 2\varepsilon_{\text{m}})^2 + \varepsilon_2^2} \quad \text{(S2)}$$

Wherein C_{abs} is the absorption cross section and C_{sca} is the scattering cross section, R is the particle radius, ε_m is the dielectric constant of the medium, ε_1 and ε_2 are the real part and imaginary part of the complex dielectric function of the particle, respectively. The complex dielectric function is approximated by the Drude model as shown in equations S2-S5,[2, 3, 7, 8]

$$\varepsilon = \varepsilon_1 + i\varepsilon_2 \quad \text{(S3)}$$

$$\varepsilon_1 = \varepsilon_\infty - \frac{\omega_{\text{p}}}{\omega^2 + \tau^2} \quad \text{(S4)}$$

$$\varepsilon_2 = \frac{\omega_{\text{p}}^2 \tau}{\left(\omega^2 + \tau^2\right)\omega} \quad \text{(S5)}$$

In which ω_p is the bulk plasma frequency of $Cu_{2-x}S_ySe_{1-y}$, τ is the free carrier damping, ε_∞ is the high-energy dielectric constant and ω is light frequency.

To extract ε_∞, ω_p, and τ, the experimental extinction cross sections were fitted to those computed via equations S2-S5, using Matlab 7.0. The experimental data was fitted through

simultaneous optimization of the relevant parameters with the Particle Swarm Optimization algorithm (PSO).[9, 10]

The free carrier density N is then obtained from the fitted plasma frequency *via* equation S6:

$$\omega_p^2 = \frac{Ne^2}{\varepsilon_0 m^*} \tag{S6}$$

Wherein e is the elementary charge, ε_0 is the permittivity of free space, and m^* is the hole effective mass. For sample N1($Cu_{0.97}S$), m^* was approximated as $0.8m_o$, where m_o is the electron mass.[2] For sample N5 ($Cu_{1.86}Se$), m^* was approximated as $0.4\ m_o$.[2] For samples N2-N4, we simply used the average of these values, $0.6m_o$.

3. *RESULTS*

3.1 Characterization of the CuCNCs with different copper deficiency

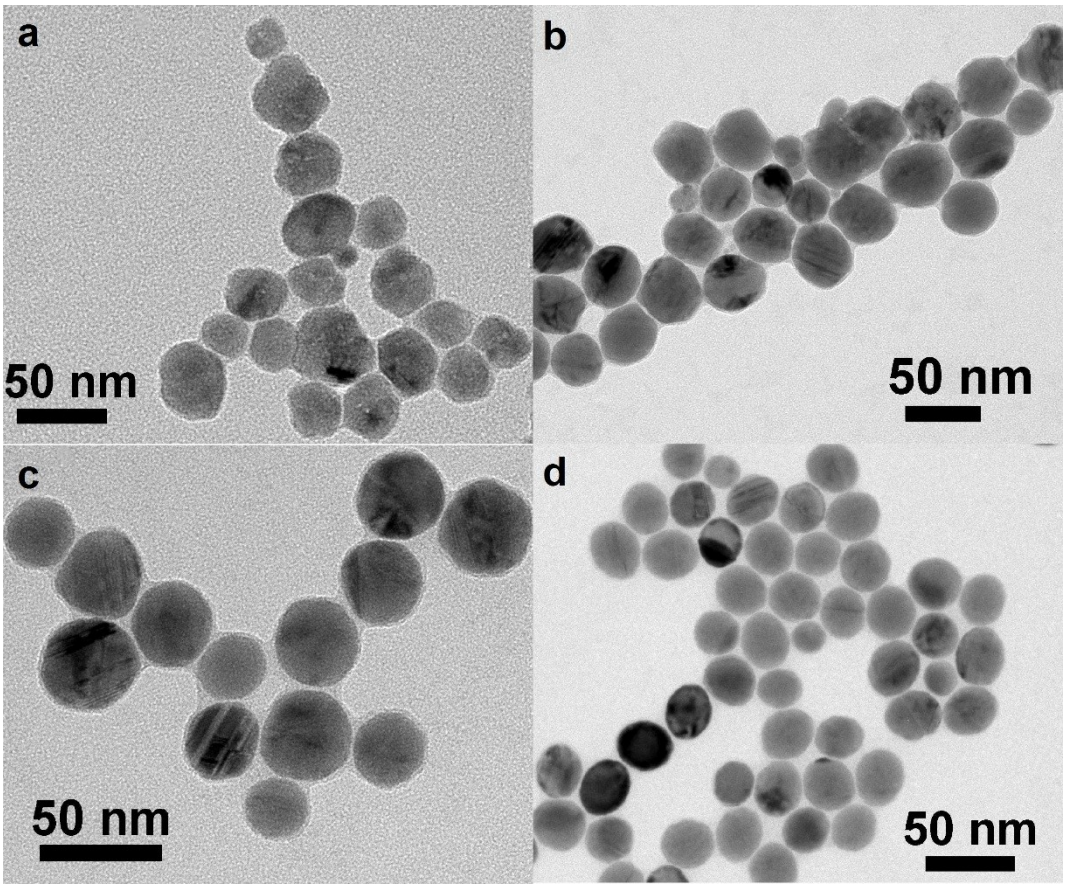

Figure S1. TEM images of $Cu_{2-x}S_ySe_{1-y}$ NCs prepared using various Se/S ratios: a) N1, 0:1; b) N2, 1:2; c) N4, 2:1; d) N5, 1:0.

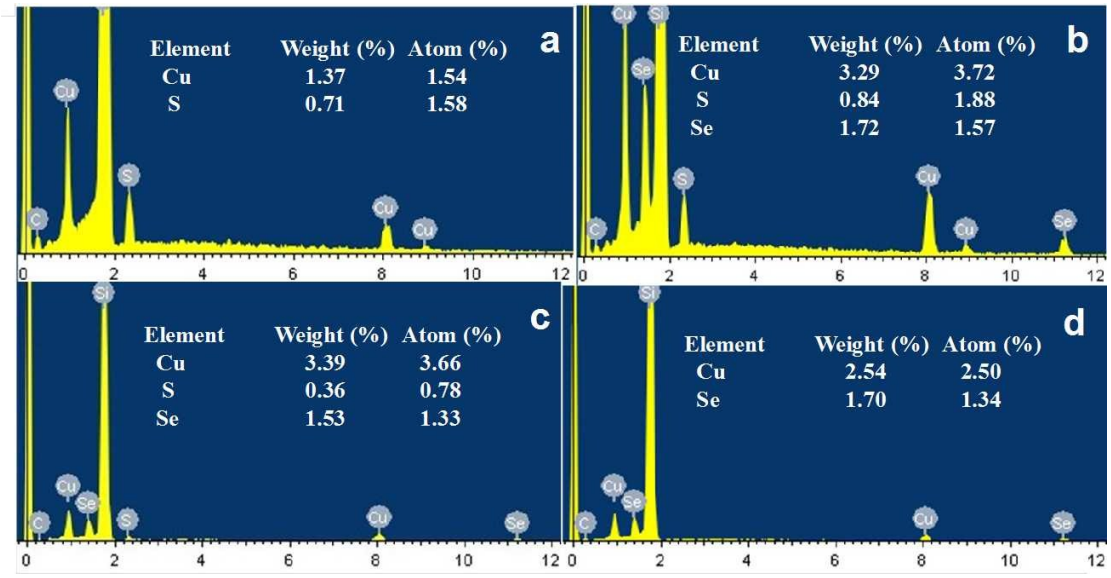

Figure S2. SEM-EDXS spectra of $Cu_{2-x}S_ySe_{1-y}$ NCs with various Se/S ratios: a) N1,0:1; b) N2, 1:2; c) N4, 2:1; d) N5, 1:0.

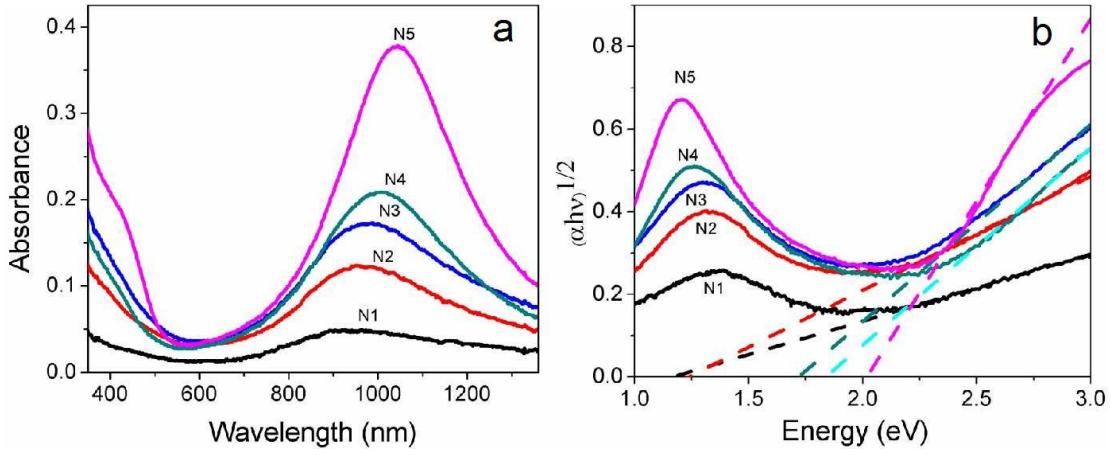

Figure S3. Extinction spectra of the nonstoichiometric copper chalcogenides nanocrystals. a) LSPR spectra of $Cu_{2-x}S_ySe_{1-y}$ NCs with various Se/S ratios: 0:1, 1:2, 1:1, 2:1, 1:0 (N1−N5). b) The bandgaps of $Cu_{2-x}S_ySe_{1-y}$ NCs with various Se/S ratios: 0:1, 1:2, 1:1, 2:1, 1:0 (N1−N5).

3.2. *Extinction spectra fitting using the Mie-Drude model*

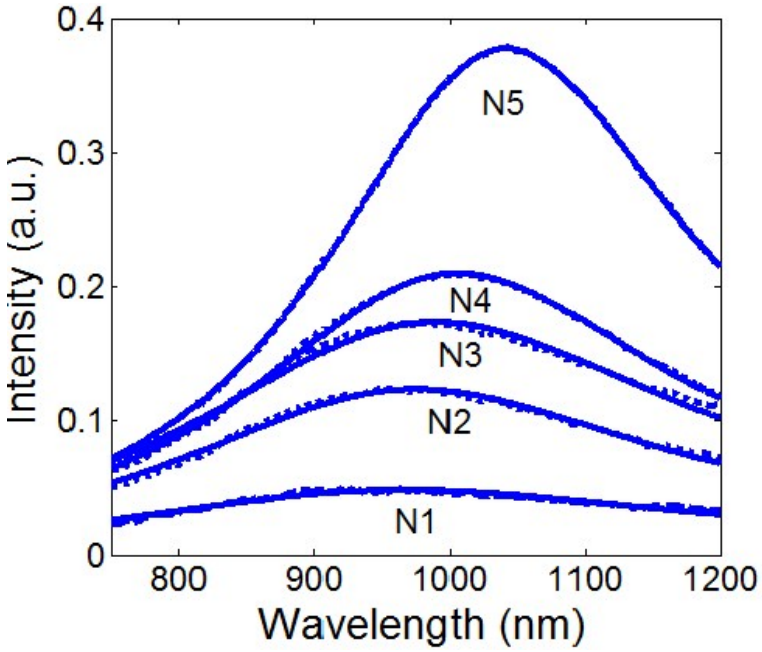

Figure S4. Extinction spectra (750−1200 nm) fitted by the Mie-Drude model. Calculated (solid line) and experimental (dotted line) extinction spectra of $Cu_{2-x}S_ySe_{1-y}$ NCs with various Se/S ratios: 0:1, 1:2, 1:1, 2:1, 1:0 (N1−N5).

3.3 NMR and MS spectra of the product of the click cycloaddition reaction

1-benzyl-4-phenyl-1H-1,2,3-triazole

Prepared following the procedure above, purified by column chromatography using aether petrolei/ethyl acetate (5:1) and isolated as a white solid. ^{1}H NMR ($CDCl_3$, 400 MHz) δ (ppm): δ7.78–7.79 (dd, J = 8.2, 1.1 Hz, 2H), 7.66 (s, 1H), 7.38–7.35 (m, 5H), 7.34–7.28 (m, 3H), 5.52 (s, 2H); ^{13}C NMR ($CDCl_3$, 100 MHz) δ 148.0, 134.6, 130.6, 129.1, 128.8, 128.1, 128.0, 125.7, 119.6, 54.2; MS (EI) m/z 236 (M+H).

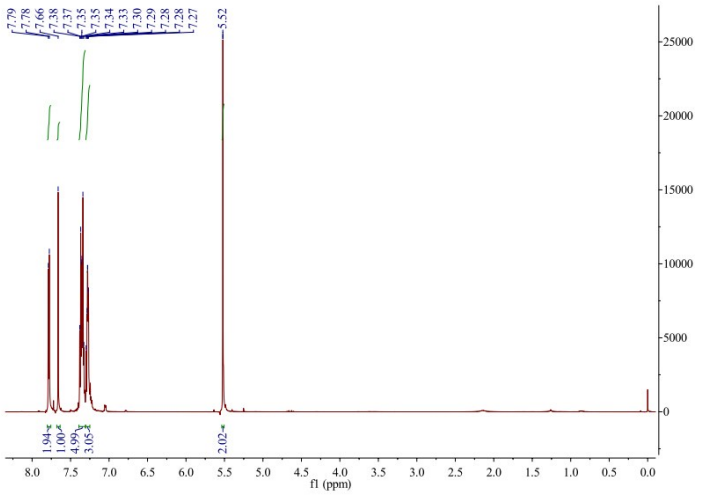

Figure S5. ^{1}H NMR spectra ($CDCl_3$, 400 MHz) of 1-benzyl-4-phenyl-1H-1,2,3-triazole.

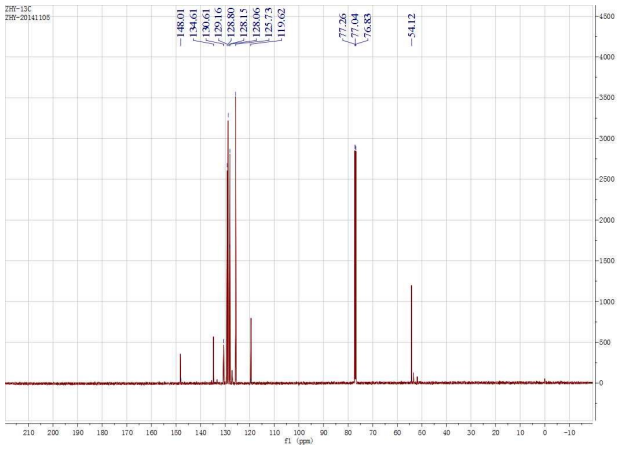

Figure S6. ^{13}C NMR spectra ($CDCl_3$, 100 MHz,) of 1-benzyl-4-phenyl-1H-1,2,3-triazole.

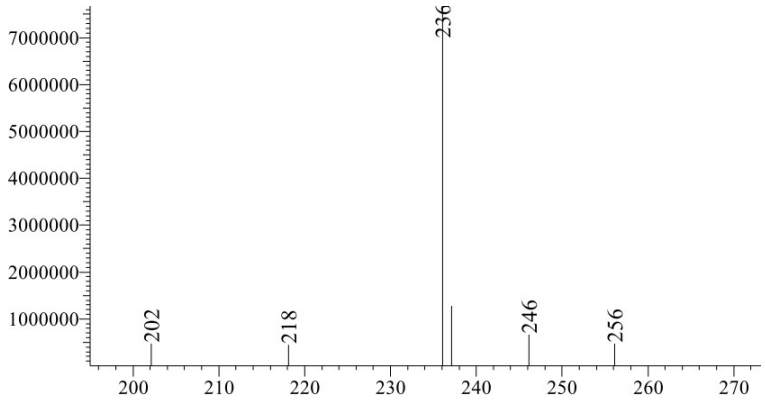

Figure S7. MS spectra of 1-benzyl-4-phenyl-1H-1,2,3-triazole.

3.4 XPS Studies of Light-controlled release of Cu(I) from $Cu_{2-x}S_ySe_{1-y}$ NCs

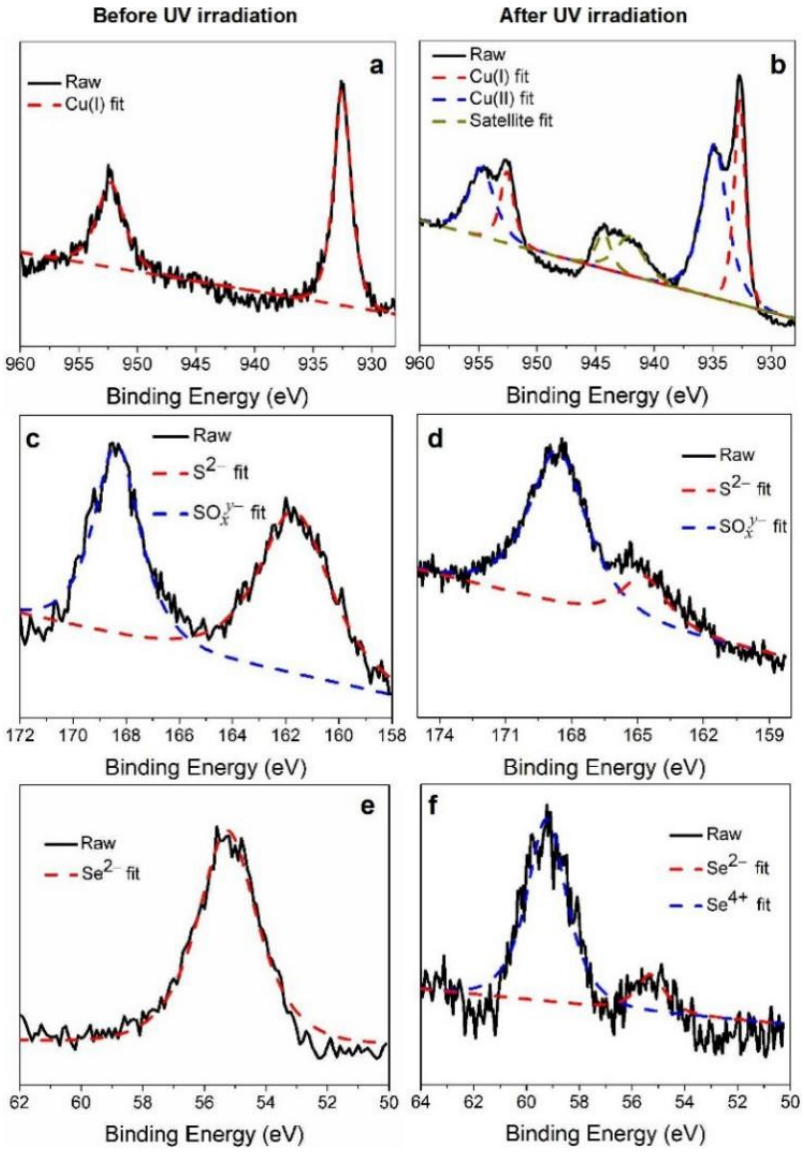

Figure S8. XPS spectra of $Cu_{1.12}S_{055}Se_{0.45}$ (N3) NCs. (a) XPS spectra of the Cu2p region as well as the Cu(I) peak fitted before UV irradiation. (b) XPS spectra of the Cu2p region as well as the Cu(I), Cu(II) and satellite peaks fitted after UV irradiation. (c) XPS spectra of the S2p region as well as the S^{2-} and SO_x^{y-} (x=3 or 4, y=2) peak fitted before UV irradiation. (d) XPS spectra of theS2p region as well as the S^{2-} and SO_x^{y-} peak fitted after UV irradiation. (e) XPS spectra of the Se3d region as well as Se^{2-} peak fitted before UV irradiation. (f) XPS spectra of Se3d region as well as Se^{2-} and Se^{4+} peaks fitted after UV irradiation.

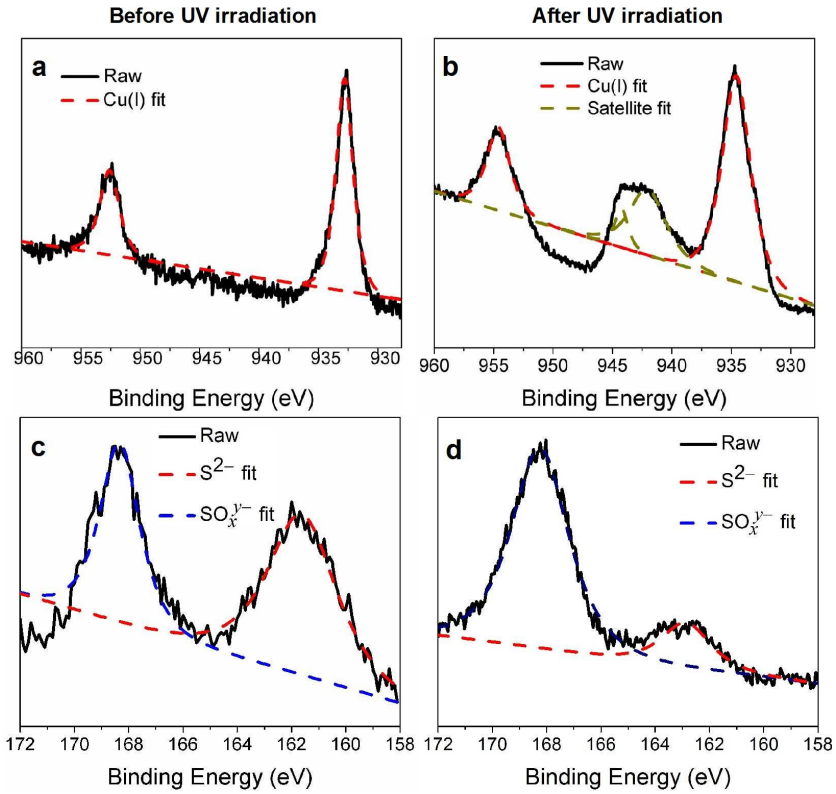

Figure S9. Changes of the XPS spectra of N1 ($Cu_{0.97}S$) before and after UV irradiation. a) XPS spectra of the Cu2p region as well as the Cu(I) peak fitted before UV irradiation; b) XPS spectra of the Cu2p region as well as the Cu(I) and satellite peaks fitted after UV irradiation; c) XPS spectra of the S2p region as well as the $S^{2-}$and SO_x^{y-} (x=3 or 4, y=2) peak fitted before UV irradiation; d) XPS spectra of the S2p region as well as the $S^{2-}$and SO_x^{y-} peaks fitted after UV irradiation.

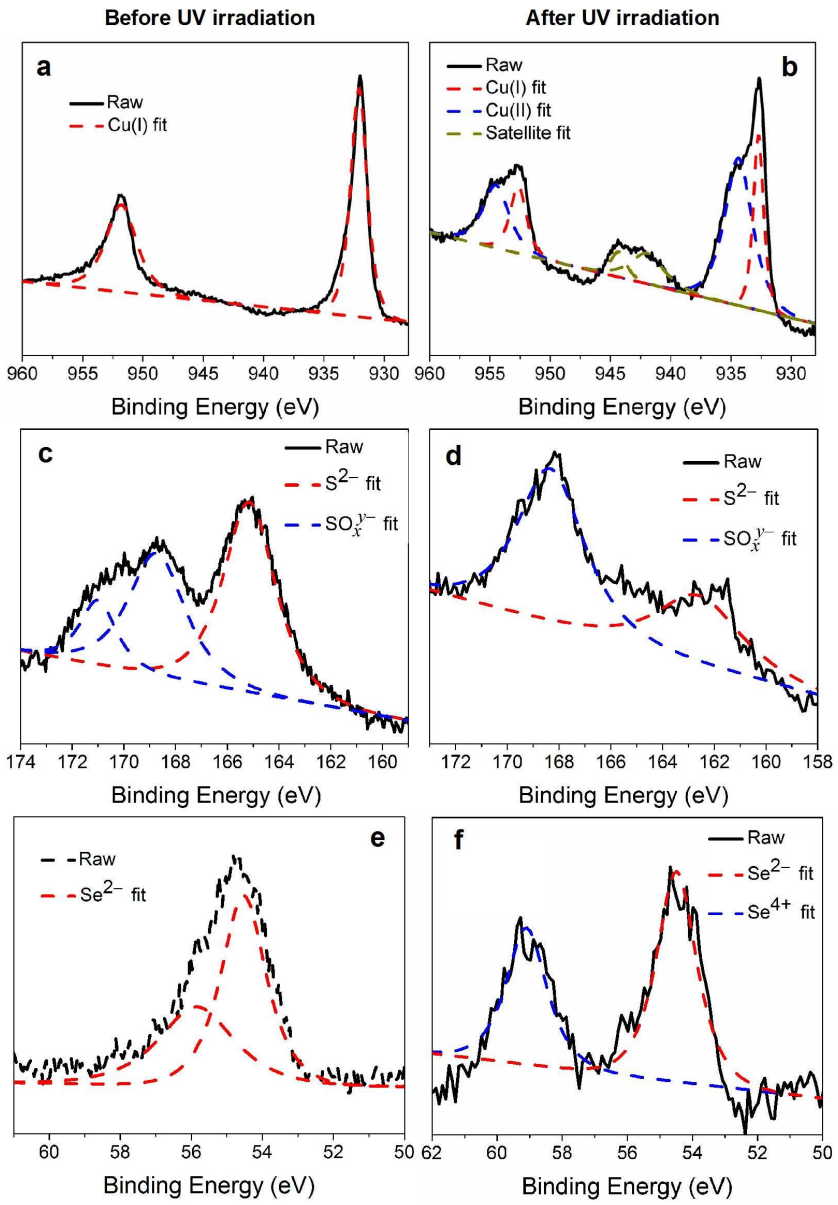

Figure S10. Changes of the XPS spectra of N2 ($Cu_{1.08}S_{0.54}Se_{0.46}$) before and after UV irradiation. a) XPS spectra of the Cu2p region as well as the Cu(I) peak fitted before UV irradiation; b) XPS spectra of the Cu2p region as well as the Cu(I), Cu(II) and satellite peaks fitted after UV irradiation; c) XPS spectra of the S2p region as well as the $S^{2-}$and SO_x^{y-} (x=3 or 4, y=2) peak fitted before UV irradiation; d) XPS spectra of the S2p region as well as the $S^{2-}$and SO_x^{y-} peak fitted after UV irradiation; e) XPS spectra of the Se3d region as well as Se^{2-} peak fitted before UV irradiation; f) XPS spectra of the Se3d region as well as Se^{2-} and Se^{4+} peaks fitted after UV irradiation.

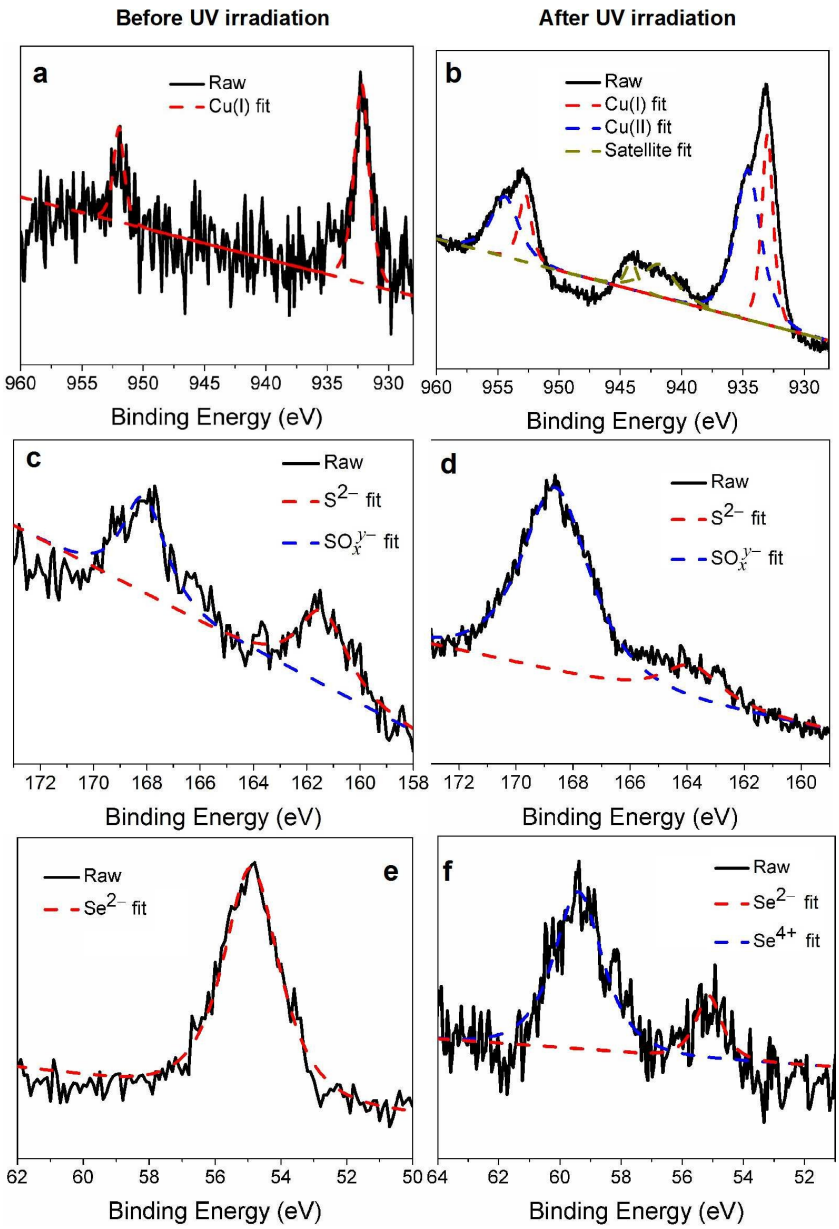

Figure S11. Changes of the XPS spectra of N4 ($Cu_{1.73}S_{0.33}Se_{0.67}$) before and after UV irradiation. a) XPS spectra of the Cu2p region as well as the Cu(I) peak fitted before UV irradiation; b) XPS spectra of the Cu2p region as well as the Cu(I), Cu(II) and satellite peaks fitted after UV irradiation; c) XPS spectra of the S2p region as well as the $S^{2-}$and SO_x^{y-} (x=3 or 4, y=2) peak fitted before UV irradiation; d) XPS spectra of theS2p region as well as the $S^{2-}$and SO_x^{y-} peak fitted after UV irradiation; e) XPS spectra of the Se3d region as well as Se^{2-} peak fitted before UV irradiation; f) XPS spectra of the Se3d region as well as Se^{2-} and Se^{4+} peaks fitted after UV irradiation.

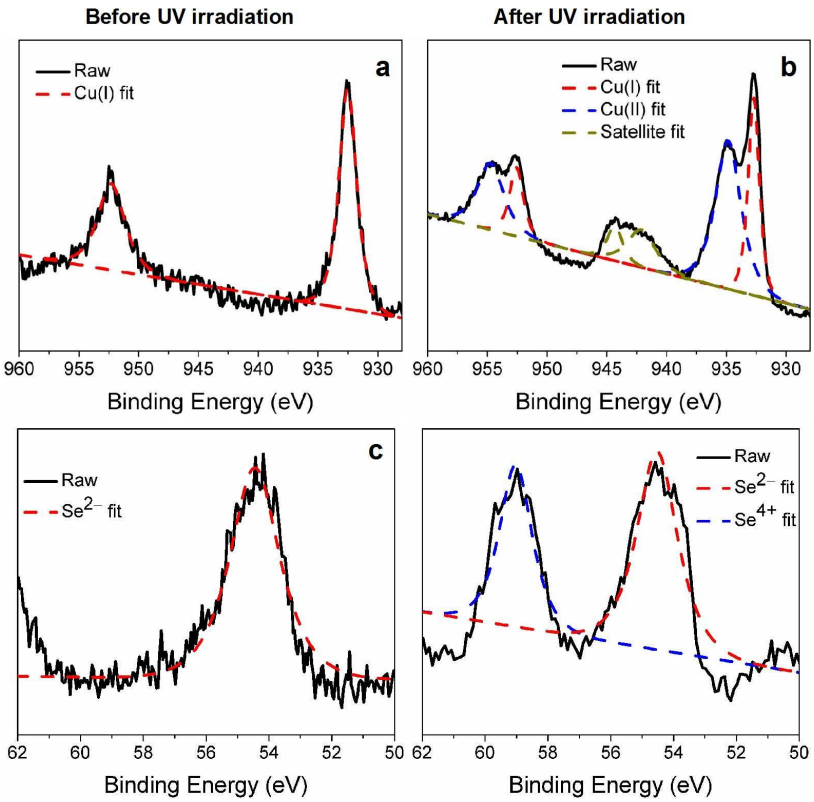

Figure S12. Changes of the XPS spectra of N5 ($Cu_{1.86}Se$) before and after UV irradiation. a) XPS spectra of the Cu2p region as well as the Cu(I) peak fitted before UV irradiation ; b) XPS spectra of the Cu2p region as well as the Cu(I), Cu(II) and satellite peaks fitted after UV irradiation; c) XPS spectra of the Se3d region as well as Se^{2-} peak fitted before UV irradiation; d) XPS spectra of the Se3d region as well as Se^{2-} and Se^{4+} peaks fitted after UV irradiation.

As shown in Figures S8-S12, the Cu2p XPS spectra after UV exposure showed pronounced satellite peaks indicative of monovalent copper with a mixture of Cu(I) and Cu(II) after UV irradiation. For S, the evolution of the S2p XPS spectra showed the molar ratio of S^{2-} to SO_x^{y-} decreased after UV irradiation. Before irradiation, Se was present only as Se^{2-}. After irradiation, some Se^{2-} was converted to Se^{4+}. Because XPS is very surface sensitive, this dramatic change in the spectra can be attributed to the oxidation of a significant portion of the surface Cu(I), resulting in the presence both Cu(I) and Cu(II). Thereby a chemical potential gradient resulted in the diffusion of Cu(I) from the particle core to the surface. Meanwhile, S and Se at the surface of the NCs were slowly photo-oxidized to SO_x^{y-} and Se^{4+} on irradiation, which caused Cu(I) to be released into solution.[11]

3.5 Light-controlled release of Cu(I) from $Cu_{2-x}S_ySe_{1-y}$ NCs as identified by ICP-AES measurements

Table S1 Amount of copper species in 0.1 mL as-synthesized $Cu_{2-x}S_ySe_{1-y}$ NCs (0.0028 M) water solution determined by ICP-AES.[a]

Entry	Amount of total Cu after UV irradiation (ng)	Amount of total Cu in the dark (ng)	Ratio of amount of total Cu
N1 (S:Se=1:0)	31.98	8.36	3.82
N2 (S:Se=2:1)	25.70	5.67	4.53
N3 (S:Se=1:1)	15.64	4.82	3.24
N4 (S:Se=1:2)	15.45	4.96	3.11
N5 (S:Se=0:1)	15.08	4.32	3.49

[a]During the measurement process, the $Cu_{2-x}S_ySe_{1-y}$ NCs in water was irradiated with 254 nm for 4 h, with the counterparts $Cu_{2-x}S_ySe_{1-y}$ suspension was kept in the dark.

3.6 Light-controlled release of Cu(I) from $Cu_{2-x}S_ySe_{1-y}$ NCs as identified by molecular absorption spectra of rhodamine B hydrazide

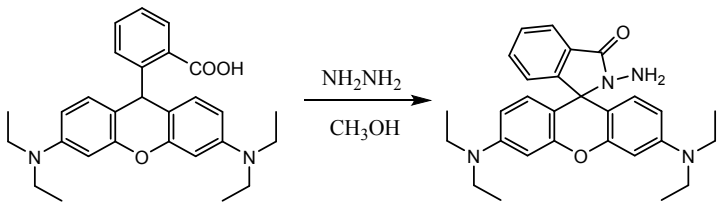

1 **2**

Rhodamine B hydrazide (**2**) was synthesized following published procedures[12] with minor modifications. Briefly, to a 100 mL flask, 1.2 g (2.5 mmol) compound **1** was dissolved in 30 mL methanol. 3.0 mL (excess) hydrazine hydrate (85%) was added dropwise under a vigorous stirring at room temperature. After that, the mixture solution was heated to 80 ^oC and refluxed for 2 hours until the solution turned light orange, and then became clear. The solvent was removed under reduced pressure. The crude product was dissolved in 50 mL 1 M HCl to generate a clear red solution and about 70 mL 1M NaOH was added into this aqueous solution slowly, with manual stirring until the solution reached pH 8−9, and a pink precipitate was formed. The final product **2** was then obtained by vacuum filtration and freeze drying.

^1H NMR ($CDCl_3$, 400 MHz) δ (ppm): 7.94 (m, 1H, Ar-H), 7.45 (m, 2H, Ar-H), 7.11 (m, 1H, Ar-H), 6.47 (m, 6H, Xanthene-H), 3.61 (b, 2H, NH_2), 3.36 (q, 8H, J = 20 Hz, NCH_2), 1.18 (t, 12H, J = 16 Hz, NCH_2CH_3).

^{13}C NMR ($CDCl_3$, 100 MHz) δ (ppm): 166.15, 153.85, 151.55, 148.91, 132.51, 130.05, 128.10, 123.83, 122.99, 108.09, 104.64, 98.03, 65.90, 44.38, 12.60.

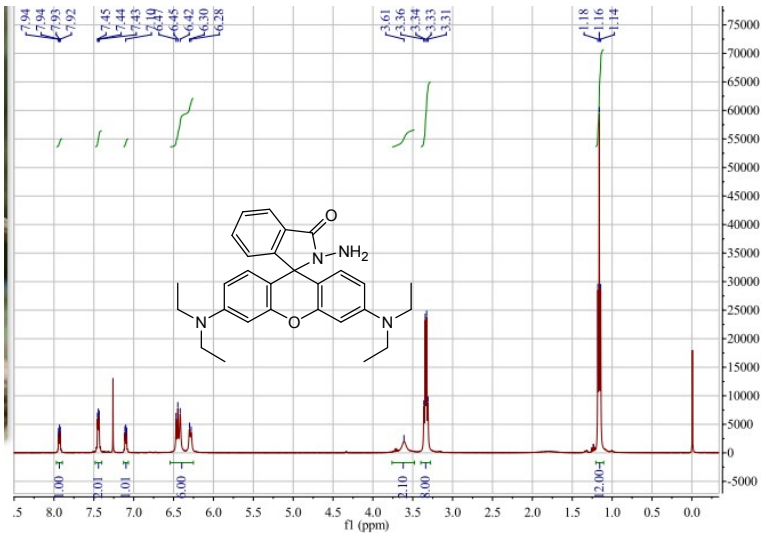

Figure S13. ^{1}H NMR spectra ($CDCl_3$, 400 MHz) of Rhodamine B hydrazide (**2**).

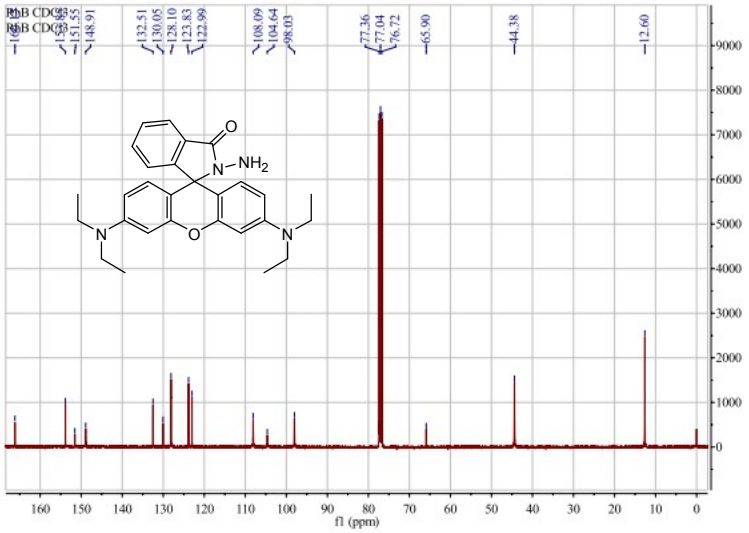

Figure S14. ^{13}C NMR spectra ($CDCl_3$, 100 MHz) of Rhodamine B hydrazide (**2**)

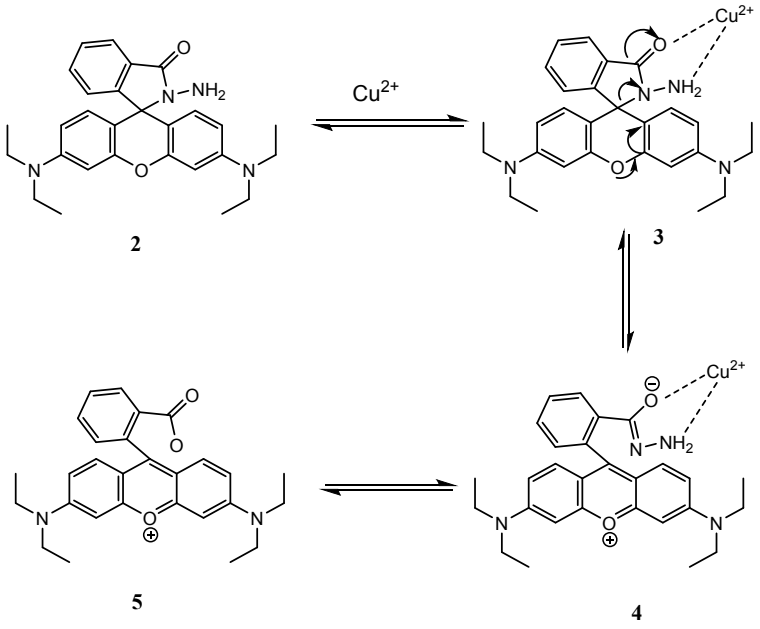

Scheme S1. The spirolactam ring-opening process of rhodamine B hydrazide (**2**) with Cu(II).[13]

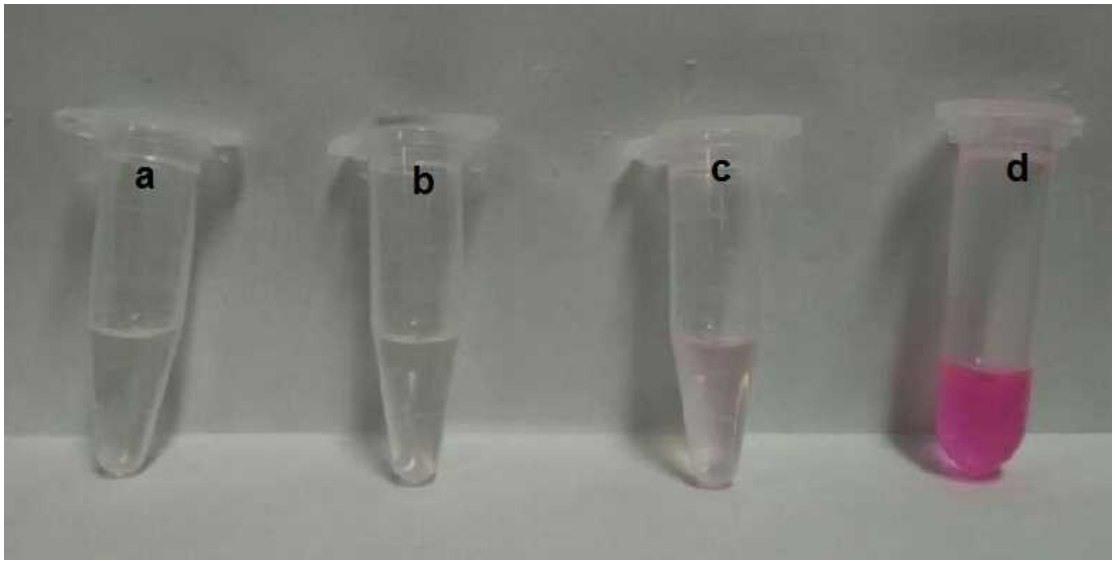

Figure S15. Investigation of Cu(II) ion by using fluorescent Rhodamine B hydrazide (**2**). a) 100 μL of the supernatant of the $Cu_{1.12}S_{0.55}Se_{0.45}$ (N3) in which total Cu concentration is 48.2 mg L^{-1} was added to compound **2** before UV irradiation. b) 100 μL of the supernatant of the UV irradiated N3 (total Cu concentration 156.4 mg L^{-1}) was added to compound **2**. c) The same amount Cu as b) from $Cu(SO_4)_2$ was added to compound **2**. d) 100 μL of C_{cu}=469.0 mg L^{-1} was added to compound **2**. All the solution was diluted to 500 μL.

Rhodamine B hydrazide employed to identify the oxidation state of the released Cu species showed that the spirolactam ring in the colorless rhodamine B hydrazide was opened in the presence of Cu(II), producing a fluorescent pink product (Scheme S1, Figure S14). This ring opening does not occur in the presence of Cu(I).[13] When the CuCNCs and rhodamine B hydrazide were illuminated, the solution remained colorless, indicating that no spirolactam ring opening occurred (Figures S14a−14c). In contrast, the colorless solution turned red when $Cu(SO_4)_2$ containing the amount of Cu released from the CuCNCs, as measured by ICP-AES above was added (Figure S14d), indicating that Cu(I) was the main species released from the NCs under illumination.

3.7 Light-controlled release of Cu(I) from $Cu_{2-x}S_ySe_{1-y}$ NCs as identified by ESR

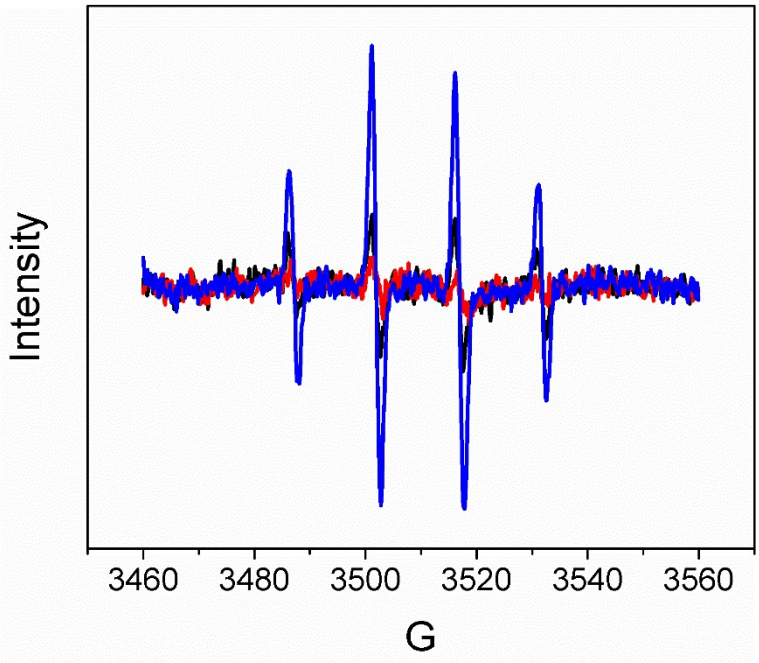

Figure S16. ESR spectra of OH· radicals generated by the nitrone spin trap 5,5-Dimethyl-1-Pyroline-N-Oxide (DMPO)-H_2O_2 system in the absence (red line) or presence (black line: before UV irradiation, blue line: after UV irradiation) of $Cu_{1.12}S_{0.55}Se_{0.45}$ (N3). Conditions: modulation amplitude, 1.944 G; microwave power, 1.002e + 001 mW; receiver gain, 1.00e + 005; sweep width, 100.00 G. The ESR measurements were achieved with a Bruker ESP-300E spectrometer operating in the X-band at room temperature.

3.8 Investigation of the kinetics of the click reaction catalyzed by $Cu_{2-x}S_ySe_{1-y}$ *NCs under varied illumination conditions*

3.8.1 Kinetic study

In an ordinary glass vial equipped with a magnetic stirring bar containing 0.07 μmol of catalyst in solvent (1 mL), was added 0.25 mmol of benzyl azide and 0.45 mmol of phenyl acetylene and the reaction mixture was stirred at 25 °C. Aliquots were taken at fixed intervals from the reaction, filtered to remove the catalyst and ^{1}HNMR employed to calculate the conversion. The equation (S7, S8) was used for calculation of rate constant *k* as below,[14, 15]

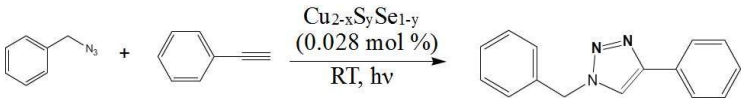

t=0	*a*	*b*	*0*
t=*t*	*a-x*	*b-x*	*x*

a=initial concentration of benzyl azide;
b=initial concentration of phenyl acetylene;
x= concentration of the product at time *t*.

Thus the rate, which is the product of the reactants, namely, *k*[benzyl azide][phenyl acetylene], can be expressed as:

$$\begin{aligned} &= -\frac{d[\text{benzyl azide}]}{dt} \\ &= -\frac{d[\text{phenyl acetylene}]}{dt} \\ &= -\frac{d(a-x)}{dt} = -\frac{d(b-x)}{dt} \\ &= k(a-x)(b-x) \end{aligned} \qquad \text{(S7)}$$

Then

$$\begin{aligned} &\frac{dx}{dt} = k(a-x)(b-x) \\ &\int \frac{dx}{(a-x)(b-x)} = \int k dt \\ &k = \frac{1}{t(a-b)} \ln\left[\frac{b(a-x)}{a(b-x)}\right] \end{aligned} \qquad \text{(S8)}$$

3.8.2 *Dynamic reaction for click chemistry catalyzed by* $Cu_{2-x}S_ySe_{1-y}$ *NCs under 100 mW/cm*^{2} *LED irradiation*

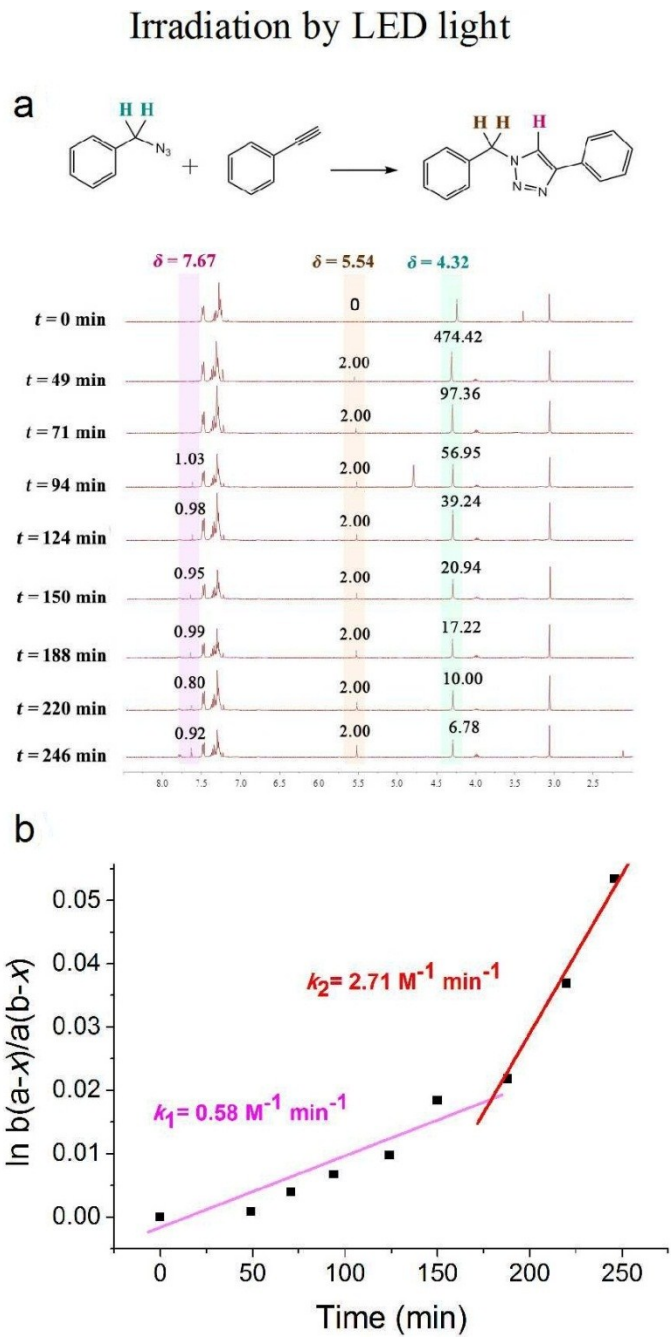

Figure S17. a)Real time ^{1}H NMR spectra of photo-CuAAC reaction between 0.25 mmol of benzyl azide and 0.45 mmol of phenyl acetylene in water catalyzed by 0.07 μmol of sample N3 under 100 mW/cm^2 LED irradiation. And b) the kinetic study was investigated using equation S7 and S8. There were two stages (k_1<k_2) and no induction period in the reaction process, suggesting quick release of Cu(I) species has occurred.

3.8.3 *Dynamic reaction for click chemistry catalyzed by* $Cu_{2-x}S_ySe_{1-y}$ *NCs in the dark*

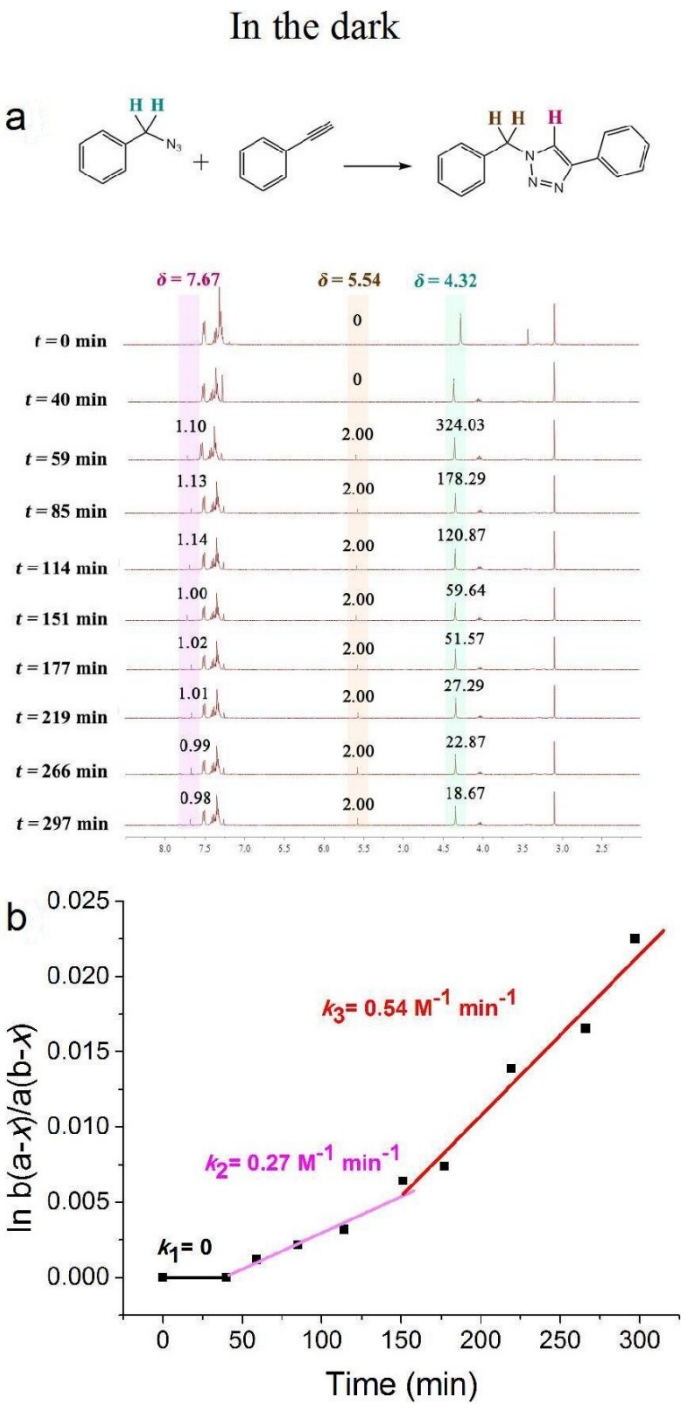

Figure S18. a) Real time ^{1}H NMR spectra of photo-CuAAC reaction between 0.25 mmol of benzyl azide and 0.45 mmol of phenyl acetylene in water catalyzed by 0.07 µmol of sample N3 in the dark. And b) the kinetic study was investigated by equation S7 and S8. There were three stages (k_1<k_2<k_3) in the reaction process. The black line (the first period) showed the long induction period (k_1=0) and slow activation of the catalyst in the dark.

3.8.4 *Dynamic reaction for click chemistry catalyzed by* $Cu_{2-x}S_ySe_{1-y}$ *NCs under the natural light*

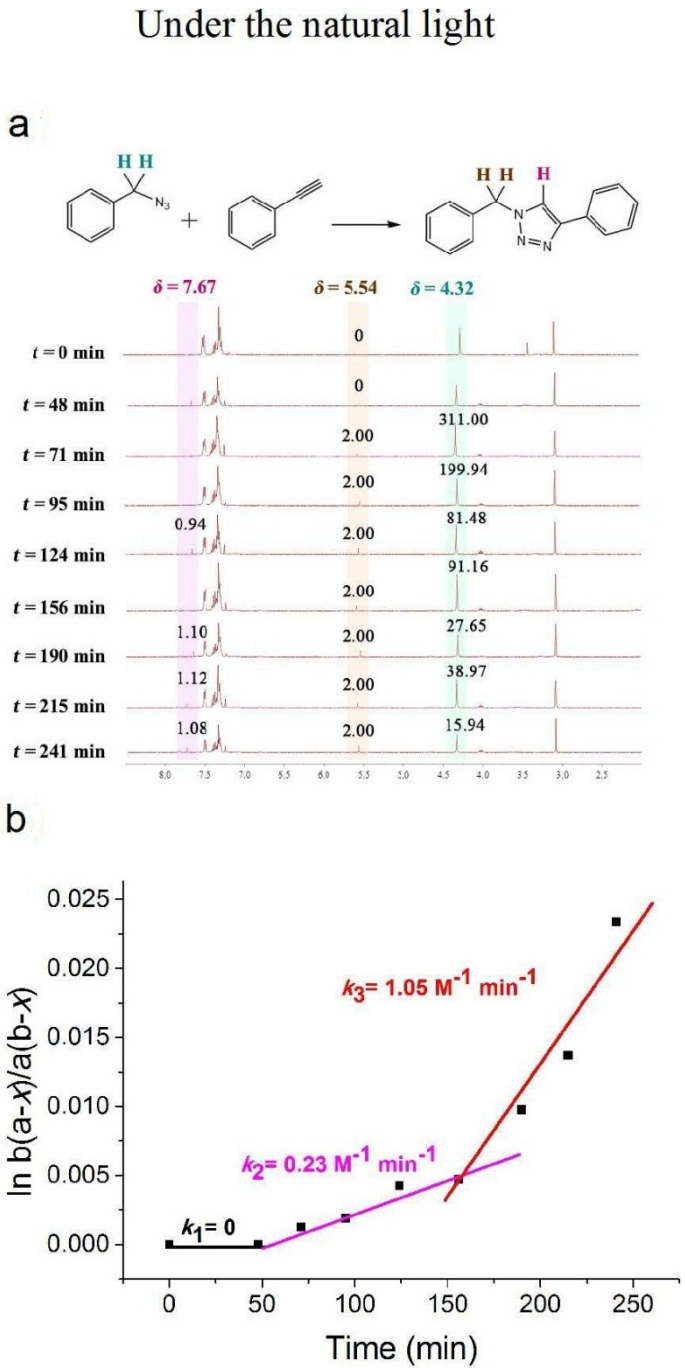

Figure S19. a) Real time ^{1}H NMR spectra of photo-CuAAC reaction between 0.25 mmol of benzyl azide and 0.45 mmol of phenyl acetylene in water catalyzed by 0.07 μmol of sample N3 under natural light. And b) the kinetic study was investigated by equation S7 and S8. There were three stages (k_1<k_2<k_3) in the reaction process. The black line (the first period) showed the long induction period(k_1=0) and slow activation of the catalyst under natural light.

3.9 Recyclability of the nonstoichiometric CuNCs for the click reactions

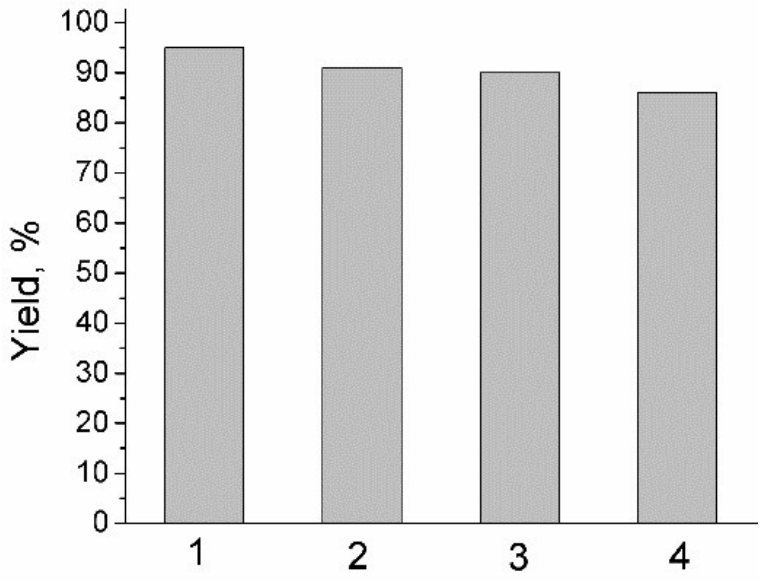

Figure S20. Recyclability of the catalysts. Isolated yields by column chromatography (silica gel column, mixture of aether petrolei/ethyl acetate=5:1 as mobile phase).

3.10 Broadening the scope of functional group for azides and alkynes

3.10.1 General synthesis of 3b-3e

In a glass vial equipped with a magnetic stir bar, 0.25 mmol benzyl azide and 0.45 mmol (1.8 equiv) ethyl propiolate, 3-butyn-2-ol, 2-fluorophenylacetylene and 3-butynyl p-toluenesulfonate was added to 1 mL $Cu_{2-x}S_ySe_{1-y}$ water solution and the reaction mixture was stirred at 25 °C. Reaction progress was monitored by TLC. For 3b, the final product was obtained by vacuum filtration and freeze drying (56.5 mg, yield: 94%). For 3c, the crude reaction mixtures were exacted by dichloromethane, and then pure click products were obtained by column chromatography (silica gel column, PE:EA=5:1 as mobile phase. 42.5 mg, yield: 80%). For 3d, the crude reaction mixtures were exacted by dichloromethane, and then pure click products were obtained by column chromatography (silica gel column, PE:EA =5:1 as mobile phase. 38.0 mg, yield: 58%). For 3e, the crude reaction mixtures were exacted by dichloromethane, and then pure click products were obtained by column chromatography (silica gel column, PE:EA =1:1 as mobile phase. 85.3 mg, yield: 93%)

ethyl 1-benzyl-1H-1,2,3-triazole-4-carboxylate (3b) 1H NMR (CDCl3, 400 MHz): δ (ppm) = 8.51 (s,

1H), 7.38 (m, 5H), 5.64 (s, 1H), 4.38 (q, 2H, *J* = 20 Hz), 1.37 (t, 3H, J = 16 Hz); 13C NMR (CDCl3, 100 MHz) δ (ppm): 160.52, 139.69, 134.85, 128.72, 128.40, 128.06, 127.86, 60.86, 53.78, 13.12.

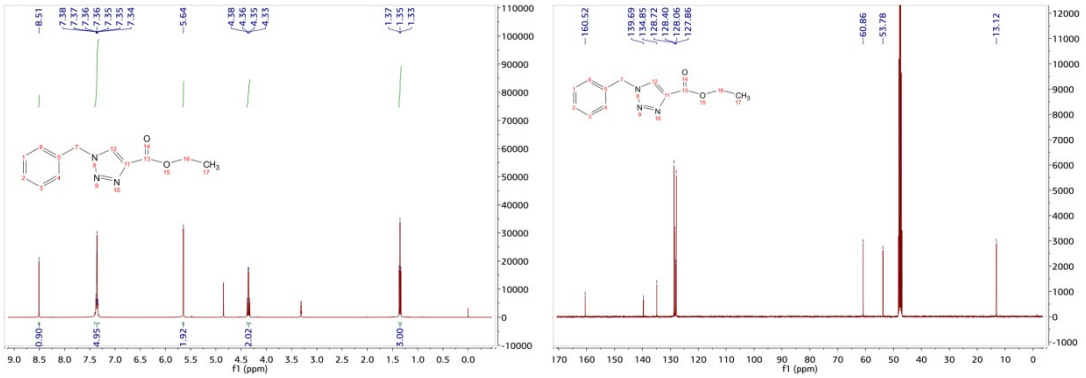

Figure S21. ^{1}H NMR and ^{13}C NMR spectra of ethyl 1-benzyl-1H-1,2,3-triazole-4-carboxylate (3b).

1-(1-benzyl-1H-1,2,3-triazol-4-yl)ethan-1-ol (3c) 1H NMR (CDCl3, 400 MHz): δ (ppm) = 7.40 (s, 1H), 7.36 (m, 5H), 5.47 (s, 2H), 5.06 (q, 1H, *J* = 20 Hz), 3.17 (b, 1H), 1.54 (d, 3H, *J* = 8 Hz); 13C NMR (CDCl3, 100 MHz) δ (ppm): 152.91, 134.60, 129.09, 128.72, 128.11, 120.10, 62.93, 54.14, 23.10.

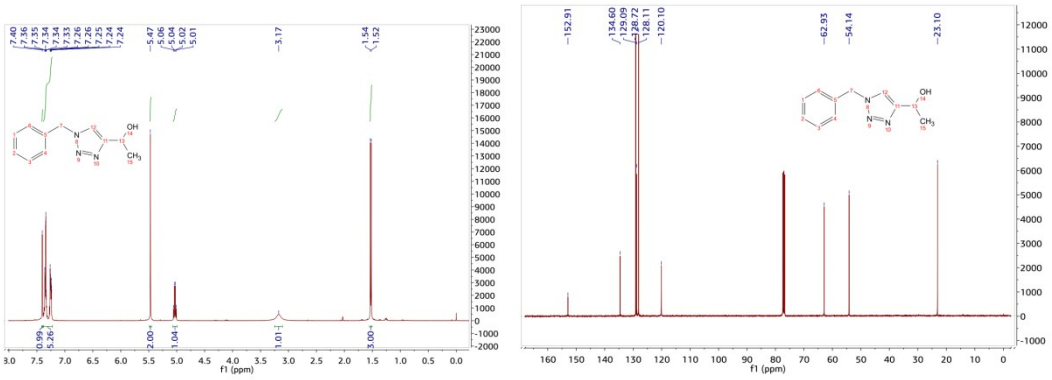

Figure S22. ^{1}H NMR and ^{13}C NMR spectra of 1-(1-benzyl-1H-1,2,3-triazol-4-yl)ethan-1-ol (3c).

1-benzyl-4-(2-fluorophenyl)-1H-1,2,3-triazole (3d) ^{1}H NMR ($CDCl_3$, 400 MHz): $\delta_{(ppm)}$ = 8.31 (t, 1H, *J* = 20 Hz), 7.86 (s, 1H), 7.39 (m, 7H), 7.24 (m, 1H), 5.59 (s, 2H); ^{13}C NMR ($CDCl_3$, 100 MHz) $\delta_{(ppm)}$: 157.98,141.66, 134.70, 129.32, 129.24, 129.13, 128.75, 127.98, 127.85, 127.81, 124.60, 122.71, 118.66, 115.71, 54.22.

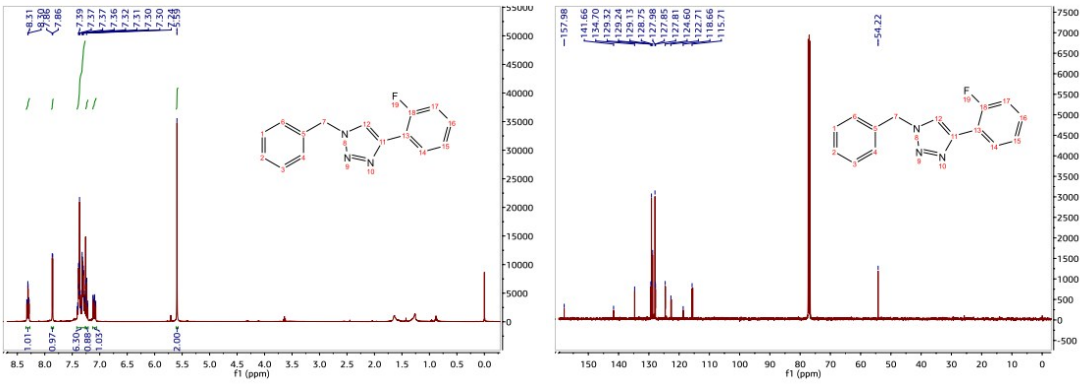

Figure S23. ^{1}H NMR and ^{13}C NMR spectra of 1-benzyl-4-(2-fluorophenyl)-1H-1,2,3-triazole (3d).

2-(1-benzyl-1H-1,2,3-triazol-4-yl)ethyl 4-methylbenzenesulfonate (3e) ^{1}H NMR ($CDCl_3$, 400 MHz): $\delta_{(ppm)}$ = 7.71 (d, 2H, *J* = 8 Hz), 7.38 (m, 3H), 7.31 (m, 5H), 5.48 (s, 2H), 4.28 (t, 2H, *J* = 16 Hz), 3.08 (t, 2H, *J* = 12 Hz), 2.43 (s, 3H); ^{13}C NMR ($CDCl_3$, 100 MHz) $\delta_{(ppm)}$:144.89, 143.17, 134.66, 132.83, 129.87, 129.12, 128.76, 128.02, 127.85, 121.93, 68.93, 54.11, 25.92, 21.62.

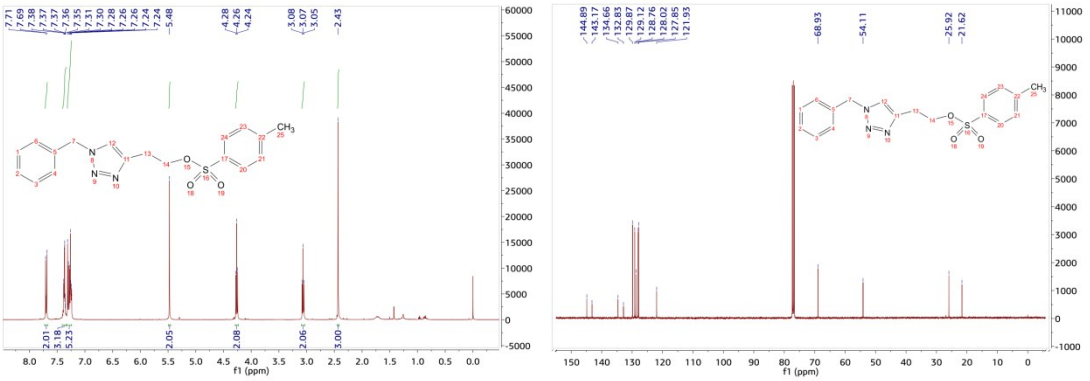

Figure S24. ^{1}H NMR and ^{13}C NMR spectra of 2-(1-benzyl-1H-1,2,3-triazol-4-yl)ethyl 4-methylbenzenesulfonate (3e).

3.10.2 *Procedure for synthesizing the azide rhodanmine B derivative*

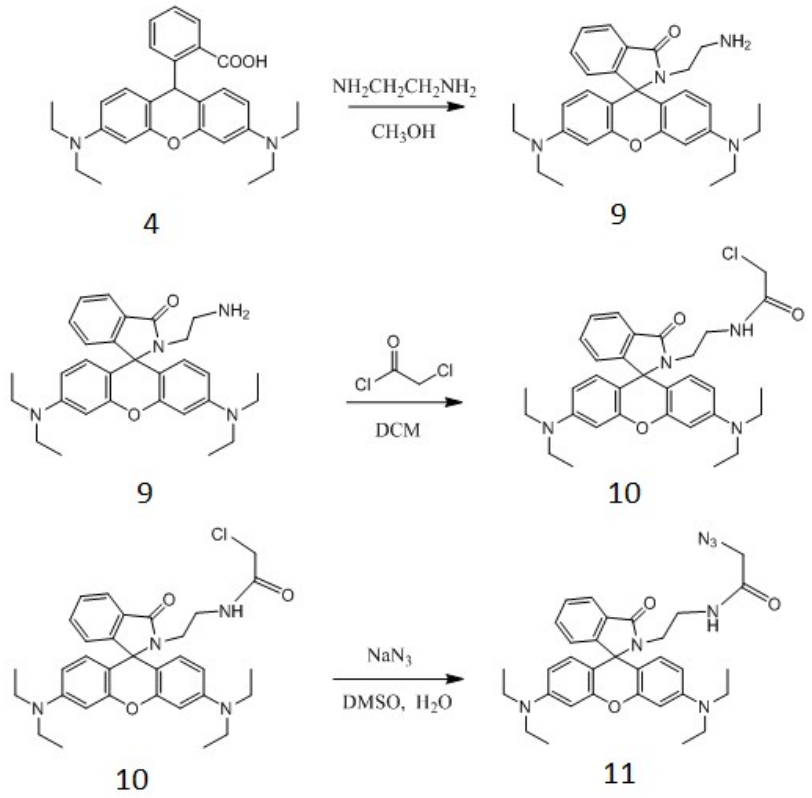

Synthesis of *N*-(rhodamine B)lactam-ethylenediamine (9). Rhodamine B (1g, 2 mmol) was dissolved in 20 mL methanol. Then ethylenediamine (1.8 mL, 2.7 mmol) was added in the solution dropwise. The mixture was stirred at reflux for 24 h until it turned orange and clear. The methanol was vacuum evaporated and left an orange viscous liquid. The crude product was dissolved in 100 mL 1 M HCl to generate a clear red solution and about 120 mL 1M NaOH was added into this aqueous solution slowly, with hand stirring until the solution reached pH 8−9, and a pink precipitate was formed. Then the final product was obtained by vacuum filtration and freeze drying (compound **9**, 1.02 g, yield: 93%).

^{1}H NMR ($CDCl_3$, 400 MHz): $\delta_{(ppm)}$ = 7.90 (s, 1H), 7.45 (s, 2H), 7.09 (s, 1H), 6.44 (m, 6H), 3.34 (d, 8H, *J* = 20 Hz), 3.19 (s, 2H), 2.41 (s, 2H), 1.58 (b, 2H), 1.18 (t, 12H, *J* = 12 Hz); ^{13}C NMR ($CDCl_3$, 100 MHz) $\delta_{(ppm)}$: 168.67, 153.49, 153.31, 148.86, 132.41, 131.25, 128.69, 128.06, 123.84, 122.78, 108.19, 105.70, 97.77, 64.98, 44.36, 43.84, 40.81, 12.60.

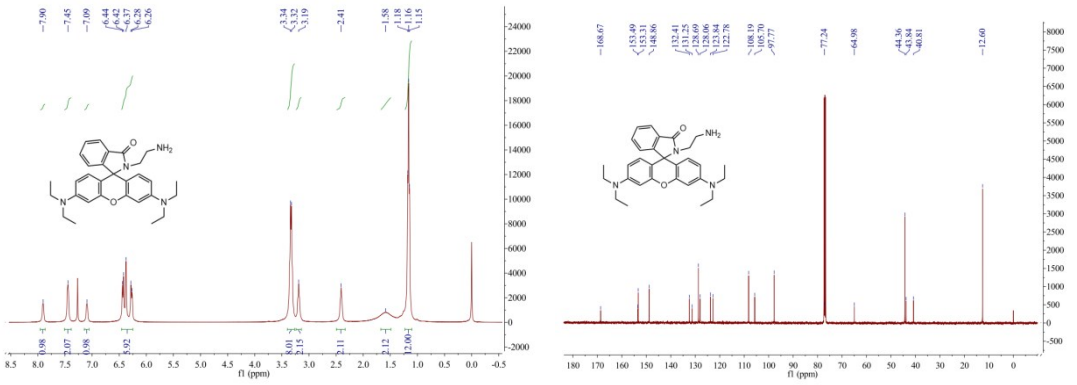

Figure S25. ^{1}H NMR and ^{13}C NMR spectra of *N*-(rhodamine B)lactam-ethylenediamine (9).

***N*-(Rhodamine-B)lactam-ethyl-2-chloroacetamide (10).** In a 100 mL dry flask, 0.968g (2 mmol) *N*-(rhodamine B)lactam-ethylenediamine (**9**) was dissolved in 20 mL of anhydrous dichloromethane. Then the solution was cooled to 0 ^{o}C. 2-chloroacetyl chloride (200 μL, sllight excess) was dissolved in 5 mL anhydrous dichloromethane and added dropwise to the flask with vigorous stirring. The mixture allowed to react for 2 h until the color changed from light yellow to orange. Then 0.1 M NaOH (about 8 mL) was added under stirring to adjust the pH to 8-9. The product was extracted with CH_2Cl_2. The organic phase was washed with water and brine three times, then dried over anhydrous Na_2SO_4. After vacuum evaporatin of the solvent, the white product (compound **7**, 0.97 g, yield: 86%) was purified by column chromatography (silica gel, PE : EA = 1 :1).

^{1}H NMR ($CDCl_3$, 400 MHz): $\delta_{(ppm)}$ = 7.93 (d, 1H, *J* = 4 Hz), 7.72 (b, 1H), 7.47 (m, 2H), 7.10 (m, 1H), 6.45 (d, 2H, *J* = 12 Hz), 6.38 (d, 2H, *J* = 4 Hz), 6.29 (dd, 2H, J_1 = 4 Hz, J_2 = 4 Hz), 3.93 (s, 2H), 3.36 (q, 10H, *J* = 20 Hz), 3.11 (m,2H), 1.19 (t, 12H, *J* = 16 Hz; ^{13}C NMR ($CDCl_3$, 100 MHz) $\delta_{(ppm)}$: 169.69, 166.28, 153.75, 153.12, 148.98, 132.78, 130.54, 128.46, 128.19, 123.91, 122.99, 108.31, 104.81, 97.82, 65.62, 52.68, 44.37, 40.54, 39.76, 12.61; FT-IR (v, cm^{-1}): 3309.85, 3078.39 (-CONH-), 786.96 (-CH_2-Cl).

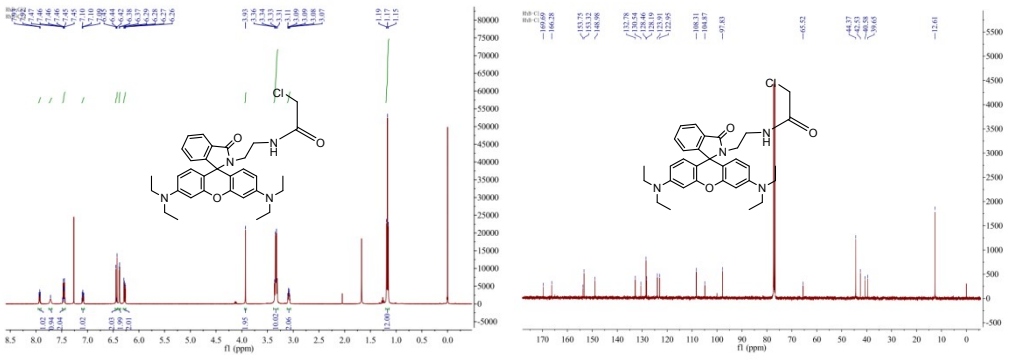

Figure S26. ^{1}H NMR and ^{13}C NMR spectra of *N*-(Rhodamine-B)lactam-ethyl-2-chloroacetamide (**10**).

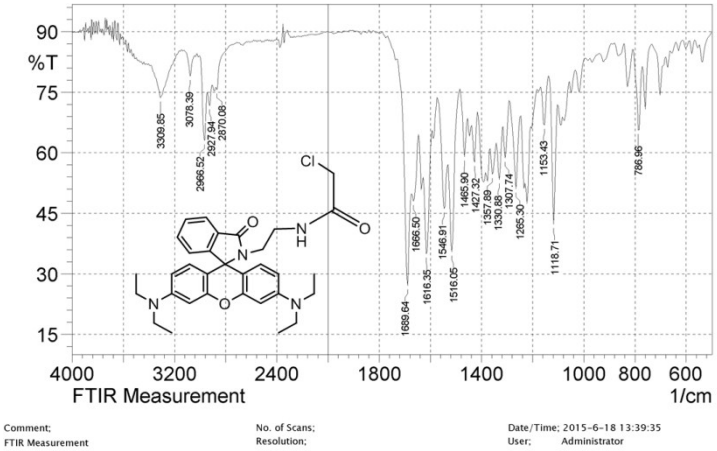

Figure S27. FTIR spectra of *N*-(Rhodamine-B)lactam-ethyl-2-chloroacetamide (**10**).

***N*-(Rhodamine-B)lactam-ethyl-2-azideacetamide (11).** In a 150 mL flask, 0.561g (1 mmol) *N*-(Rhodamine-B)lactam-ethyl-2-chloroacetamide (**10**) was dissolved in the mixture of 50 mL DMSO and 25 mL water. Sodium azide (280 mg, 4 mmol) and a catalytic amount of KI were added in the solution. The mixture was refluxed and stirred for 24 h. Then the product was extracted with ethyl ether. The organic phase was washed with water and brine three times, then dried over anhydrous Na_2SO_4. After vacuum evaporation of the solvent, the white product was obtained without a need for further purification (compound **11**, 0.553 g, yield: 97%).

^{1}H NMR ($CDCl_3$, 400 MHz): $\delta_{(ppm)}$ = 7.94 (m, 1H), 7.60 (b, 1H), 7.47 (m, 2H), 7.10 (m, 1H), 6.44 (d, 2H, J = 8 Hz), 6.38 (d, 2H, J = 4 Hz), 6.29 (dd, 2H, J_1 = 4 Hz, J_2 = 4 Hz), 3.82 (s, 2H), 3.36 (m, 10H), 3.08 (q, 2H, J = 16 Hz), 1.19 (t, 12H, J = 16 Hz); ^{13}C NMR ($CDCl_3$, 100 MHz) $\delta_{(ppm)}$: 169.88, 166.91, 153.73, 153.33, 149.00, 132.82, 130.50, 128.44, 128.21, 123.91, 122.99, 108.31, 104.81, 97.82, 65.62, 52.68, 44.37, 40.54, 39.76, 12.61; FT-IR (v, cm^{-1}): 2106.27 (-N_3), 621.08 (-CH_2-N_3).

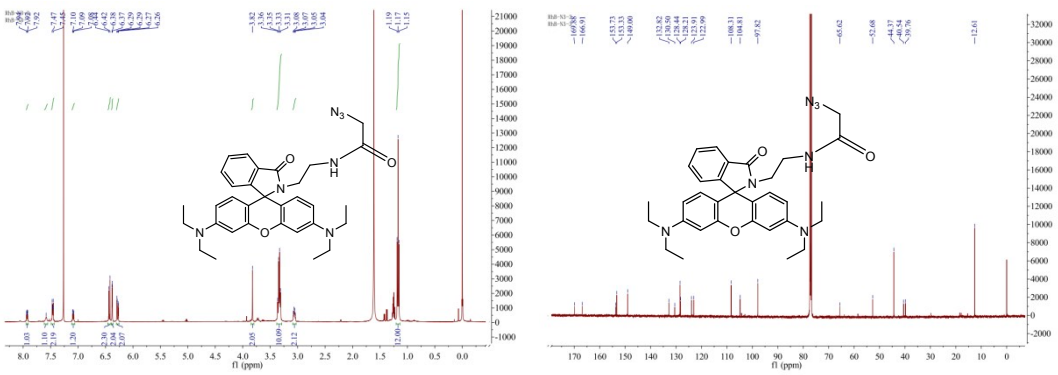

Figure S28. ^{1}H NMR and ^{13}C NMR spectra of *N*-(Rhodamine-B)lactam-ethyl-2-azideacetamide (**11**).

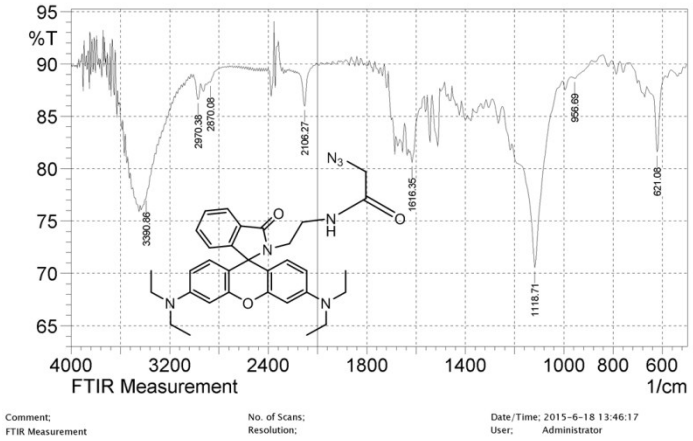

Figure S29. FTIR spectra of *N*-(Rhodamine-B)lactam-ethyl-2-azideacetamide (**11**).

***N*-(Rhodamine-B)lactam-ethyl-2-(4-phenyl-1H-1,2,3-triazol-1-yl)acetamide (3f).**

In a 25 mL flask, 0.067 g (0.12 mmol) N-(Rhodamine-B)lactam-ethyl-2-azideacetamide (**11**) and 20 μL (0.18 mmol) phenylacetylene were dissolved in 15 mL methanol and 7 nmol $Cu_{2-x}S_ySe_{1-y}$ NCs as catalyst was added in the mixture. The reaction mixture was stirred for 10 hours under UV light in room temperature. After vacuum evaporation of the solvent, the white product (compound **3f**, 0.058 g, yield: 72%) was purified by column chromatography (silica gel, PE : EA = 1 :1).

^{1}H NMR ($CDCl_3$, 400 MHz): $\delta_{(ppm)}$ = 7.99 (s, 1H), 7.80 (m, 3H), 7.45 (m, 5H), 7.06 (d, 1H, *J* = 8 Hz), 6.67 (b, 1H), 6.35 (d, 2H, *J* = 4 Hz), 6.29 (m, 4H), 5.03 (s, 2H), 3.34 (q, 10H, *J* = 20 Hz), 2.95 (q, 2H, *J* = 12 Hz), 1.17 (t, 12H, *J* = 16 Hz); ^{13}C NMR ($CDCl_3$, 100 MHz) $\delta_{(ppm)}$: 169.55, 165.10, 153.33, 153.27, 149.00, 148.31, 132.80, 130.43, 128.79, 128.26, 128.18, 125.86, 122.83, 121.32, 108.40, 104.83, 97.70, 65.26, 52.93, 44.37, 39.95, 39.10, 12.56.

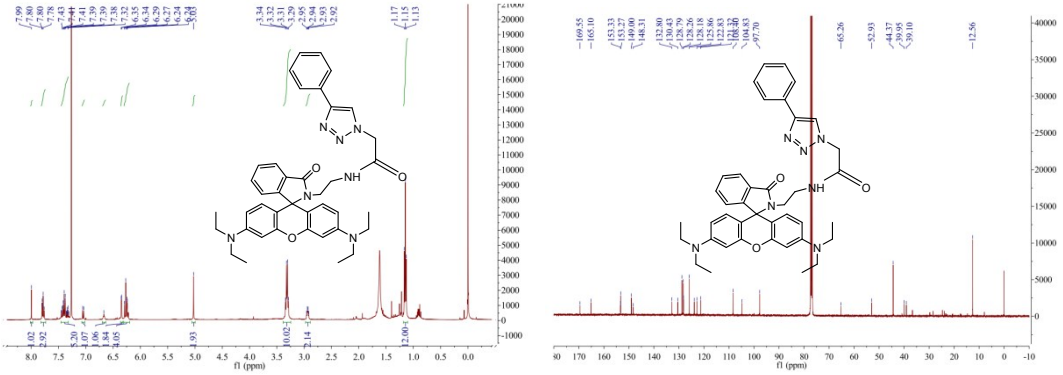

Figure S30. ^{1}H NMR and ^{13}C NMR spectra of *N*-(Rhodamine-B)lactam-ethyl-2-(4-phenyl-1H-1,2,3-triazol-1-yl)acetamide (**3f**).

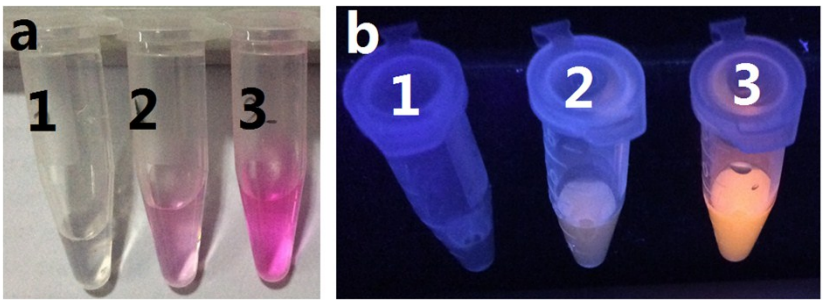

Figure S31. Equilibrium investigation of *N*-(Rhodamine-B)lactam-ethyl-2-azideacetamide (**11**). a) Photograph of microcentrifuge tubes in which 100 μM of $CuCl_2$ (2) or 100 μM of ascorbic acid (3) was added to the compound **11**. A clear pink color could be observed, in contrast to the compound **11** solution alone (1). b) Photograph of the same samples under UV illumination. Clear orange fluorescence is observed in samples 2 and 3, in contrast to the pure compound **11** solution (1).

3.11 Investigation of the cytotoxicity of $Cu_{2-x}S_ySe_{1-y}$ NCs

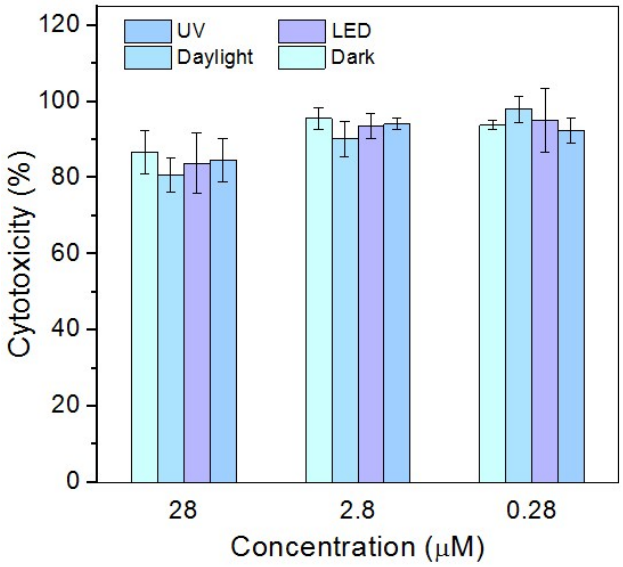

Figure S32. Cell viability in the presence of the $Cu_{2-x}S_ySe_{1-y}$ (sample N3) at varying concentrations after different light irradiation.

4. REFERENCES

1. J. Tauc, *Mater. Res. Bull*. 1970, **5**, 721–729.
2. F. Scotognella, G. Della Valle, A. R. S. Kandada, M. Zavelani- Rossi, S. Longhi, G. Lanzani, and F. Tassone, *Eur. Phys. J. B.* 2013, **86**, 154.
3. J. M. Luther, P. K. Jain, T. Ewers and A. P. Alivisatos, *Nat. Mater*. 2011, **10**, 361–366.

4. F. Scotognella, D. V. Giuseppe, R. S. K. jay, D. Dirk, Z. Margherita, C. Matteo, M. Karol, C. Alberto, K. Kseniya, L. Guglielmo, M. Liberato and T. Francesco. *Nano Lett*. 2011, **11**, 4711–4717
5. Y H. J.ang, C. Y. Chen, F. W.Yuan and H. Y. Tuan, *J. Phys. Chem. C* 2013, **117**, 21955–21964.
6. X. Liu and M. T. Swihart, *Chem. Soc. Rev*. 2014, **43**, 3908–3920.
7. Y. Xie, L. Carbone, C. Nobile, V. Grillo, S. D'Agostino, F. D. Sala, C. Giannini, D. Altamura, C. Oelsner, C. Kryschi and P. D. Cozzoli, *ACS Nano* 2013, **7**, 7352–7369.
8. I. Kriegel, J. Rodríguez-Fernández, A. Wisnet, H. Zhang, C. Waurisch, A. Eychmüller, A. Dubavik, A. O. Govorov and J. Feldmann, A*CS Nano*, 2013, **7,** 4367–4377.
9. J. Kennedy and R. Eberhart, Proceedings of the IEEE International Conference on Neural Networks, Perth, Australia, IEEE Service Center, Piscataway, NJ, 1995, **4**, 1942–1948.
10. H. Y. Zou, H. L.Wu, H. Y. Fu, L. J. Tang, L. Xu, J. F. Nie and R. Q. Yu, *Talanta,* 2010, **80**, 1698–1701.
11. J. J.Wang, D. J. Xue, Y. G. Guo, J. S. Hu and L. J.Wan, *J. Am. Chem. Soc*. 2011, **133**, 18558–18561.
12. Y. Xiang, A. Tong, P. Jin and Y. Ju, *Org. Lett*. 2006, **8**, 2863–2866.
13. V. Dujols, F. Ford and A. W. Czarnik, *J. Am. Chem. Soc*. 1997, **119**, 7386–7387.
14. V. O. Rodionov, V. V. Fokin and M. G. Finn, *Angew. Chem.* 2005, **117**, 2250–2255.
15. A. S. Nia, S. Rana, D. Döhler, X. Noirfalise, A. Belfiore, W. H. Binder, C*hem. Commun*. 2014, **50**, 15374–15377.